

Article (refereed) - postprint

Rowe, E.C.; Tipping, E.; Posch, M.; Oulehle, Filip; Cooper, D.M.; Jones, T.G.; Burden, A.; Hall, J.; Evans, C.D. 2014. **Predicting nitrogen and acidity effects on long-term dynamics of dissolved organic matter.**

Copyright © 2013 Elsevier Ltd.

This version available <http://nora.nerc.ac.uk/500590/>

NERC has developed NORA to enable users to access research outputs wholly or partially funded by NERC. Copyright and other rights for material on this site are retained by the rights owners. Users should read the terms and conditions of use of this material at <http://nora.nerc.ac.uk/policies.html#access>

NOTICE: this is the author's version of a work that was accepted for publication in *Environmental Pollution*. Changes resulting from the publishing process, such as peer review, editing, corrections, structural formatting, and other quality control mechanisms may not be reflected in this document. Changes may have been made to this work since it was submitted for publication. A definitive version was subsequently published in *Environmental Pollution* (2014), 184. 271-282. [10.1016/j.envpol.2013.08.023](https://doi.org/10.1016/j.envpol.2013.08.023)

www.elsevier.com/

Contact CEH NORA team at
noraceh@ceh.ac.uk

Predicting nitrogen and acidity effects on long-term dynamics of dissolved organic matter

Rowe EC ^{*1}, Tipping E ², Posch M ³, Oulehle F ^{1,4}, Cooper DM ¹, Jones TG ⁵, Burden A ¹, Monteith DT ², Hall J¹ & Evans CD ¹

* Corresponding author. Email: ecro@ceh.ac.uk. Postal address: Centre for Ecology and Hydrology, ECW, Deiniol Road, Bangor, LL57 2UW, UK.

¹ Centre for Ecology and Hydrology, ECW, Deiniol Road, Bangor, LL57 2UW, UK.

² Centre for Ecology and Hydrology, LEC, Library Avenue, Lancaster, LA1 4AP, UK.

³ Coordination Centre for Effects (CCE) at RIVM, P.O. Box 1, NL-3720 BA Bilthoven, Netherlands.

⁴ Czech Geological Survey, Geologická 6, 152 00 Praha 5, Czech Republic.

⁵ School of Biological Sciences, Bangor University, Deiniol Road, Bangor, LL57 2UW, UK

Target Journal: Environmental Pollution

Suggested referees:

1. Werner Borken, Soil Ecology, University of Bayreuth, Germany. werner.borken@uni-bayreuth.de
2. Heleen de Wit, Norwegian Institute for Water Research. heleen.de.wit@niva.no
3. Steven Perakis, USGS, 3200 SW Jefferson Way, Corvallis, OR 97331, USA. sperakis@usgs.gov
4. Martin Forsius, Finnish Environment Institute, P.O. Box 140, 00251 Helsinki, Finland. martin.forsius@ymparisto.fi
5. Martyn Fitter, Swedish University of Agricultural Sciences, Box 7050, Lennart Hjelm's väg 9, 750 07 UPPSALA, Sweden. martyn.fitter@slu.se

Abstract

Increases in dissolved organic carbon (DOC) fluxes may relate to changes in sulphur and nitrogen pollution. We integrated existing models of vegetation growth and soil organic matter turnover, acid-base dynamics, and organic matter mobility, to form the 'MADOC' model. After calibrating parameters governing interactions between pH and DOC dissolution using control treatments on two field experiments, MADOC reproduced responses of pH and DOC to additions of acidifying and alkalising solutions. Long-term trends in a range of acid waters were also reproduced. The model suggests that the sustained nature of observed DOC increases can best be explained by a continuously replenishing potentially-dissolved carbon pool, rather than dissolution of a large accumulated store. The simulations informed the development of hypotheses that: DOC increase is related to plant productivity increase as well as to pH change; DOC increases due to nitrogen pollution will become evident, and be sustained, after soil pH has stabilised.

Keywords: DOC, dynamic models, carbon, soil, nitrogen

44

45 **Introduction**

46

47 Observed increases in dissolved organic carbon (DOC) concentration in many north-temperate
48 surface waters (Evans et al., 2005; Findlay, 2005; Oulehle and Hruska, 2009) may indicate changes in
49 soil carbon storage (Freeman et al., 2001), and give rise to increased water treatment costs (Chow et
50 al., 2003). These increases have been attributed to various factors (Clark et al., 2010), such as pH
51 increase resulting mainly from a decline in sulphur (S) pollution (De Wit et al., 2007; Evans et al.,
52 2006; Evans et al., 2008a; Haaland et al., 2010; Monteith et al., 2007; SanClements et al., 2012);
53 climate change (Freeman et al., 2001); nitrogen enrichment (Bragazza et al., 2006; Findlay, 2005;
54 Pregitzer et al., 2004); changes in precipitation patterns (Hongve et al., 2004; Ledesma et al., 2012);
55 or changes in management such as burning (Clutterbuck and Yallop, 2010; Holden et al., 2012).
56 While it is doubtful that all of these proposed drivers have combined to cause an increase in DOC in
57 all locations, it is likely that interactions among some factors, in particular acidification recovery and
58 factors affecting plant productivity, will affect DOC fluxes. Several models of DOC dynamics have
59 been developed (Futter et al., 2007; Jutras et al., 2011; Michalzik et al., 2003; Neff and Asner, 2001;
60 Xu et al., 2012) but these generally focus on seasonal dynamics and require detailed inputs
61 describing hydrological processes. There remains a need for a simple model, which simulates long-
62 term controls on DOC fluxes and is suitable for large-scale applications. In the current study, we
63 summarised key processes affecting DOC into a simple annual-timestep model, and applied this to
64 experimental and long-term monitoring studies in which DOC and acid-base dynamics could be
65 related.

66

67 Dissolved organic matter is defined as particles that pass through a 0.45 µm filter (Sleutel et al.,
68 2009), and includes molecules of 100 to 100,000 Da (Aitkenhead-Peterson et al., 2003) with variable
69 C/N ratio and surface charge. The formation and loss of DOC are affected by biological and surface
70 exchange processes. The sorption and flocculation of potentially-dissolved organic carbon (PDOC) is
71 mediated by hydrophobicity, ligand exchange between surface hydroxyl groups and organic acids,
72 electrostatic interactions, and coadsorption and competition with other anions (Tipping, 1990).
73 Several of these processes are influenced by soil solution acidity. At low pH, much low-molecular-
74 weight organic matter stays in the solid phase, flocculated or adsorbed onto larger particles, in
75 particular iron and/or aluminium oxyhydroxides (Sleutel et al., 2009). As pH increases, this organic
76 matter tends to de-flocculate and desorb. In solution, acid groups on DOC partially buffer pH
77 increases (Evans et al., 2008b; Krug and Frink, 1983).

78

79 Fluxes of DOC are greater from more organic soils, and correlate well with soil total C/N ratio
80 (Aitkenhead-Peterson et al., 2005; van den Berg et al., 2012). Concentrations of DOC are determined
81 not simply by soil solution acidity but also by the dynamics of soil C. During decomposition, DOC is
82 produced by the action of microorganisms on plant litter and soil organic matter. Decomposition in
83 organic soils is commonly impeded by anaerobic conditions, and may only proceed as far as soluble
84 forms of C. Studies of ¹⁴C concentration indicate that much of the DOC in streams (Raymond et al.,
85 2007; Tipping et al., 2010) and in peat pipes (Billett et al., 2012) results from recent inputs of plant-
86 derived C. This recent origin implies that, other factors being equal, DOC concentrations are likely to
87 be correlated with plant productivity. This inference is supported by the conclusion of Larsen et al.
88 (2011a) from a study of Norwegian lakes that a correlation of DOC concentration with temperature
89 was primarily due to increased vegetation cover. In a related study, by far the best predictor of lake
90 DOC concentration among a set of catchment properties that included annual mean temperature,
91 slope, and fractions of bog, forest and arable land, was the normalised-difference vegetation index,
92 which indicates photosynthetic capacity (Larsen et al., 2011b). Evidence that DOC fluxes are
93 correlated more strongly with solar radiation 1-2 months previously than with air or soil
94 temperature (Harrison et al., 2008) also indicates the importance of recently fixed C.

95
96 Nitrogen deposition has variable effects on DOC flux. It has been suggested that N pollution will
97 increase DOC flux due to the suppression of phenol oxidase activity by nitrate (DeForest et al., 2004),
98 but no evidence was found for this effect in an experimental study (DeForest et al., 2005). Increased
99 N deposition has been observed to decrease (De Wit et al., 2007), increase (Filep and Rekasi, 2011),
100 or have no net effect on (Emmett et al., 1998; Fernandez and Rustad, 1990; Stuanes and Kjonaas,
101 1998) DOC flux. None of these studies reported effects on plant productivity, so it is difficult to judge
102 which of these systems was N-limited. Productivity is limited by N supply in many terrestrial
103 ecosystems, since N is energetically expensive to obtain through fixation and easily lost through
104 leaching and gaseous pathways (LeBauer and Treseder, 2008; Vitousek and Howarth, 1991), but at a
105 given site other limitations may predominate such as growing season length (Kerkhoff et al., 2005)
106 or availability of other nutrients (Menge et al., 2012). Increases in plant productivity as a result of
107 chronic pollution with reactive N have however been observed at least in the short term in many
108 forest ecosystems (Bontemps et al., 2011; Hogberg et al., 2006; Lu et al., 2012; Wei et al., 2012) and
109 are likely in other habitats where N has historically been limiting. Where increased N supply
110 increases productivity, there will potentially be an increase in DOC flux, although this also depends
111 on soil and hydrological properties that determine the retention, transport and mineralisation of
112 DOC.

113
114 Soils often change considerably in organic matter content, biotic activity and surface chemistry with
115 depth. Mineral soil horizons with large concentrations of iron and/or aluminium oxyhydroxides
116 generally have greater DOC sorption capacity than organic horizons. In a study of Belgian forests,
117 sorption was responsible for substantial retention (67-84%) of DOC entering the mineral soil profile
118 with forest floor leachate (Sleutel et al., 2009). Reductions in S pollution and sulphate concentrations
119 may free up anion exchange sites in lower soil horizons, increasing the sorption of DOC (Borken et
120 al., 2011). Much of the retained organic matter is likely to be mineralised before it can be leached,
121 resulting in lower DOC concentrations in streams than in soil solution. This process also releases
122 mineral N, which may be re-immobilised or taken up by plants, depending on the amount of labile C-
123 rich organic matter and the presence of plant roots within deeper soil layers. These processes can
124 result in considerable decoupling between fluxes of dissolved organic N (DON) and DOC (Kalbitz et
125 al., 2000).

126
127 The concentrations of DOC in rivers and lakes are affected by DOC efflux from different landscape
128 elements depending on the flow regime (Laudon et al., 2011). Flow pathways through soil vary with
129 rainfall intensity. During high-flow periods, much of the streamflow derives from near-surface
130 drainage through more organic horizons (Hagedorn et al., 2000), resulting in greater stream DOC
131 concentrations and considerably greater DOC fluxes during storm events (Buffam et al., 2001).
132 Conversely, during periods of low water flow, DOC concentrations in streams are reduced by surface
133 interactions and mineralisation within the mineral soil. As well as affecting flow pathways and (via
134 effects on anaerobiosis) DOC formation, water flux directly affects the solubilisation of DOC since
135 greater volumes of water allow more dissolution of PDOC. Thus DOC concentrations do not show a
136 strong decline with precipitation (Haaland et al., 2008; van den Berg et al., 2012), as would be
137 expected from simple dilution.

138
139 Previous approaches to modelling DOC fluxes (Futter et al., 2007; Jutras et al., 2011; Michalzik et al.,
140 2003; Xu et al., 2012) have most often focused on seasonal and episodic variation in DOC production
141 and in flow pathways through soil layers, and consequently require detailed hydrological and
142 meteorological parameterisation. For modelling long-term changes in DOC flux we assume that the
143 key processes are the production, mineralisation and solubilisation of DOC. A similar approach was
144 taken by Neff and Asner (2001), who based their DOC model on a three-pool soil C model
145 instantiated in four soil layers and with an hourly-timestep hydrology model. In the current study we

146 propose a much simpler approach to modelling DOC changes using a Model of Acidity Dynamics and
147 Organic Carbon (MADOC), developed by integrating models of: a) plant production and soil total C
148 and N dynamics; b) partitioning of DOC between solid and dissolved phases; and c) acid-base
149 kinetics. The MADOC model simulates the effects on long-term trends of DOC of large-scale
150 ecosystem drivers such as air pollution by N and S. The aim of the study was to determine whether
151 observed changes in soil solution and stream chemistry across a range of experimental and long-
152 term monitoring sites can be simulated using a combination of these relatively simple models.

153

154 **Methods**

155

156 *Model development*

157

158 Three annual-timestep models of vegetation and soil dynamics were dynamically integrated to form
159 the MADOC model: N14C (Tipping et al., 2012), VSD (Posch and Reinds, 2009), and a simplified
160 version of DyDOC (Michalzik et al., 2003). A major goal in developing the model was to limit
161 structural detail and number of parameters wherever possible, resulting in a model that is
162 generalisable and widely applicable. The model simulates dynamics within a one dimensional
163 vegetation-soil column and is suitable for simulating experimental plots, and larger-scale areas
164 where spatially-lumped parameters can be used. The integrated model was developed in Fortran90;
165 an executable version is available on request. Data for calibrating the model were obtained from
166 control treatments on experimental N addition sites, and the model was tested against data from
167 acidified and alkalisated treatments from these sites, and from long-term monitoring sites.

168

169 The VSD model (Posch and Reinds, 2009) was developed as the simplest dynamic model compatible
170 with the computation of critical loads for S and N deposition by simple mass balances (UBA, 2004),
171 and is based on solving equations that describe competition among cations for exchange sites and
172 thus the partitioning of ions between the solution and adsorbed phases. The model was run using
173 Gapon exchange kinetics. Whereas the original model assumed complete nitrification (and thus zero
174 concentration of NH_4^+ in soil solution), the version included in MADOC uses the concentrations of
175 NO_3^- and NH_4^+ supplied by the N14C model, as described below. A retained fraction of deposited S
176 can be specified to simulate retention of reduced and organic S. A version of VSD without surface
177 exchange processes was used to simulate the chemistry of subsoil solution and of surface waters.

178

179 The N14C model (Tipping et al., 2012) simulates C and N dynamics in vegetation and soils, tracking
180 three organic matter pools with mean residence times at 10 °C of 2, 20 and 1000 years. The turnover
181 of these pools is divided between a mineralisation flux (into CO_2 or inorganic N) and a proportion
182 becoming low-molecular-weight PDOM. In the version used within MADOC the proportions of C and
183 N turnover were allowed to differ, to represent uncoupling of solution DOC and DON. The year is
184 subdivided into a cold season, when mineralised N is either re-immobilised or leached, and a
185 growing season, when plant uptake can occur before immobilisation or leaching. Litterfall returns C
186 and N to the soil organic matter pool, although a vegetation-type-specific proportion of plant
187 biomass is retained from year to year.

188

189 The DyDOC model (Michalzik et al., 2003) simulates the formation, transport and retention of DOC
190 within soil profiles. We adapted the model by simplifying the original three-horizon structure and
191 removing hydrological detail. The simplified model is described below, and parameters are listed in
192 Table 1. A pool of PDOM was defined in terms of stocks of C and of N. The annual change in these
193 pools (Equations 1 and 2) was determined from input fluxes (fixed proportions of overall soil C and N
194 turnover as calculated using the N14C model), mineralisation calculated using a first-order
195 exponential function, and leaching.

196

197 [1]

198 [2]

199
200 where C_{pd} and N_{pd} are single pools of potentially-dissolved C and N in g m^{-2} , T_C and T_N are the net
201 annual turnovers of C and N in $\text{g m}^{-2} \text{ yr}^{-1}$ as calculated by the N14C model, k_{inpdC} and k_{inpdN} are the
202 proportions of these turnovers entering the potentially-dissolved pools, k_{minpd} is the rate constant for
203 mineralisation of both C_{pd} and N_{pd} pools in yr^{-1} , W_d is the water drainage flux in $\text{g m}^{-2} \text{ yr}^{-1}$, and C_{DOC}
204 and C_{DON} are concentrations in the soil solution in g g^{-1} . These concentrations were calculated from
205 the stocks of potentially-dissolved C and N, assuming that in the absence of soil the whole stock
206 would be dissolved, resulting in a concentration determined by water mass. Soil reduced this
207 concentration according to soil mass and a pH-dependent coefficient determining partitioning
208 between solid and solution phases (Equations 3 and 4).

209

210 _____ [3]

211

212 _____ [4]

213

214 where M_w is the mass of water (g m^{-2}), including both annual average water content and annual
215 drainage flux, M_s is the mass of soil (g m^{-2}), and k_D is a partitioning coefficient calculated as the
216 average coefficient for mineral and organic soil, weighted by the thickness of these horizons
217 (Equation 5).

218

219 _____ [5]

220

221 where k_{Dorg} and k_{Dmin} are partitioning coefficients for organic and mineral soil, and L_{org} and L_{min} are
222 the thicknesses in m of the organic and mineral horizons. The partitioning coefficients were
223 dependent on soil solution H^+ activity, and were calculated for organic soil (Equation 6) and mineral
224 soil (Equation 7) using different values for a partition constant.

225

226 _____ [6]

227 _____ [7]

228

229 where k_{Dorg} and k_{Dmin} are the partitioning coefficients for organic and mineral soil, α_{org} and α_{min} are
230 the partition constants ($\text{m}^3 \text{ g}^{-1} \text{ L mol}^{-1}$) for organic and mineral soil, and a_{H^+} is the soil solution H^+
231 activity (mol L^{-1}).

232

233 Quantities passing among the component models are illustrated in Figure 1. In the current study, the
234 main drivers of interest were N and S deposition. Nitrogen dynamics in soil and vegetation were
235 simulated using N14C. The original N14C model calculated a flux of DOM, which in the current model
236 was assumed to enter a PDOM pool as described above. With mineralisation of this potentially-
237 dissolved pool, there was further release of mineral N, which was then leached. The DON flux
238 calculated by MADOC was assumed not to contribute to plant uptake. Total mineral N release as
239 calculated by the N14C and DyDOC models was split between reduced and oxidised forms, using a
240 soil-type-specific constant nitrate proportion, P_{nit} . The VSD model determined ion exchange
241 dynamics according to this supply of ammonium and nitrate, deposition rates of S and other
242 elements, and DOC flux as calculated by DyDOC. A constant proportion, P_{sites} , of the DOC was
243 assumed to be able to form acid anions, i.e. a fixed value for dissociation site density. The value of
244 pH influenced DOC dissolution in the DyDOC model.

245

246 The N14C model allows for the adsorption of DOC to mineral surfaces in deeper soil horizons, using a
247 simplified version of the algorithm used for the upper horizons. Surface waters were assumed to
248 have undergone these deeper soil processes, so stream and lake DOC measurements were
249 compared with simulated DOC flux flowing from the deeper soil. Of the DOC flux from the upper
250 horizons, a proportion is assumed to bypass the deeper soil, with the remainder entering the
251 deeper-soil pool. The proportion bypassing the deeper soil pool was assumed to be one for peats
252 and gley soils, and zero for other soils. A temperature-dependent proportion of the deeper-soil pool
253 is mineralised each year, and a proportion leached. In the original N14C model this proportion was
254 fixed, but the rapid changes in UK surface-water DOC concentrations (Monteith and Evans, 2005)
255 suggest that pH changes are also affecting the subsoil sorbed C pool. The dissolution of potentially-
256 dissolved subsoil C was therefore made pH-dependent, using the same partition constant (α_{\min}) as
257 for shallower mineral soil. The DOC flux from deeper soil was converted to a concentration, based on
258 precipitation surplus, and other solute concentrations were as predicted for topsoil leachate by
259 MADOC. The pH values for the subsoil and surface waters were calculated using instances of a
260 simplified version of VSD that does not include weathering or cation exchange. To avoid the need to
261 seek solutions to simultaneous equilibria, the N14C and DyDOC models used pH values calculated for
262 the previous year.

263

264 *Data sources*

265

266 An experiment to study the effects of acid anion and base cation deposition on soil solution
267 chemistry was set up in 2007, on British upland moor sites on the Migneint range (52° 59.6' N, 3°
268 48.8'W) and in the Peak District (53° 28.3' N, 1° 54.5' W) (Evans et al., 2012b). On each site, additions
269 of acidifying solution (H₂SO₄) or alkalisng solution (mainly NaOH, with some CaCl₂, MgCl₂ and KCl)
270 were made to both peat and podzol soils, with four replicate plots. Equivalent volumes of rainwater
271 were added to control plots. The trajectories of deposition, including atmospheric and experimental
272 additions, are illustrated in Figure 2. The current study related MADOC predictions of yearly mean
273 soil solution chemistry to yearly mean soil solution measurements for each of the treatments. Soil
274 solution was sampled using suction lysimeters at 5-10 cm depth, and the simulations were run for
275 soil above 10 cm depth. The soil was organic to at least the depth of the samplers in both the peat
276 and the podzol treatments. Following calibration of the MADOC model using the control treatments
277 of the experimental study (see below), the performance of the model against an independent
278 dataset was evaluated, with minimal additional calibration. This dataset was obtained from the Acid
279 Waters Monitoring Network (AWMN), a set of 22 lakes and streams in upland areas of the UK that
280 has been monitored since 1988 (18 sites) or 1990-1991 (four sites) (Evans et al., 2010b; Monteith
281 and Evans, 2005; Patrick et al., 1991).

282

283 Present-day S and mineral N deposition estimates for all sites were obtained using CBED model
284 estimates for the years 2006-2008 (Smith et al., 2000). The history of depositions at each site after
285 1910 was estimated by scaling to historic sequences obtained using the FRAME model (Dore et al.,
286 2009). Following Tipping et al. (2012), pre-1850 N deposition was assumed to be zero, with
287 ecosystem N during this period supplied entirely from N₂ fixation at a rate of 0.3 g m⁻² yr⁻¹.
288 Atmospheric N deposition during the 1850-1910 period was assumed to increase linearly from zero
289 to the rate calculated by the deposition model for 1910.

290

291 Fixed inputs for the MADOC model are listed in Table 1, and site-specific inputs are listed in Table 2.
292 Organic acids were assumed to be triprotic, and mean values from a study by Oulehle et al. (in press)
293 were used for dissociation constants for the three protons and for P_{sites} . The partial pressure of CO₂
294 in solution in soil was assumed to be 0.037 atm, i.e. 100 times atmospheric concentration, and to
295 decline in streams to twice atmospheric concentration, and in lakes to atmospheric concentration.
296 Net plant uptake was assumed to be zero, since there was little or no harvest of nutrient elements

297 from the modelled catchments. Weathering of N, chloride (Cl^-), sulphate, phosphate and sodium
298 were assumed to be zero. The temperature range (difference between growing season and non-
299 growing season in mean temperature) was set to 7 °C for all sites. Values for several MADOC inputs
300 which are difficult to ascertain experimentally were obtained by calibrating the model to
301 observations, as described below. Values for other input parameters for the N14C submodel were as
302 described in (Tipping et al., 2012).

303

304 *Calibration of model parameters*

305

306 The model was calibrated to measurements from control treatments on the experimental sites, by
307 minimising the sum of absolute differences using the Nelder-Mead simplex method (Nelder and
308 Mead, 1965). For simultaneous calibrations to more than one type of measurement, the error for
309 each was weighted by the inverse of the mean measured value. Simulations began 12000 years
310 before present, to allow organic matter pools to stabilise. Parameter values were fitted in sequence.
311 Firstly, Cl^- deposition as estimated for each of the two sites by the CBED model was adjusted to
312 minimise error in soil solution Cl^- , assuming that Cl^- is fully conservative in the soil. Soil solution Cl^-
313 provides a proxy measurement of the deposition input which is more accurate than modelled
314 deposition estimates. The marine component of inputs of other ions was adjusted in the same ratio.
315 Next, the sodium (Na^+) weathering rate was adjusted for each site and soil type to minimise error in
316 soil solution Na^+ . The VSD parameter f_{Sret} , i.e. the proportion of S deposition that is immobilised and
317 does not contribute to SO_4^{2-} leaching, was then adjusted for each site and soil type to minimise error
318 in soil solution SO_4^{2-} . Next, the aluminium (Al^{3+}) equilibrium constants for each site and soil type
319 were adjusted to minimise error in soil solution total inorganic Al^{3+} . VSD considers exchange of
320 calcium (Ca^{2+}), magnesium (Mg^{2+}) and potassium (K^+) together, so the total weathering rate of these
321 cations for each site and soil type was adjusted to minimise error in total concentration of Ca^{2+} , Mg^{2+}
322 and K^+ . Once the simulations had been constrained to match these major ion fluxes as closely as
323 possible given sampling error in the measurements, model parameters governing organic matter
324 dynamics were adjusted. The k_{inpdN} parameter has a major influence on the long-term development
325 of soil C and N pools, and was adjusted for each site and soil type to minimise error in soil total C/N
326 ratio. To minimise error in DOC flux, firstly k_{minpd} and α_{org} were adjusted using single values for all
327 soils and sites, and then the k_{inpdC} parameter was adjusted separately for each site and soil type. The
328 DOC site density was then adjusted separately for each site and soil type to minimise error in pH.

329

330 A similar calibration procedure was followed for the AWMN sites, fitting Cl^- deposition to minimise
331 error in surface water Cl^- , Na^+ weathering to minimise error in surface water Na^+ , and f_{Sret} to
332 minimise error in surface water SO_4^{2-} . Base cation fluxes in surface water include subsoil base cation
333 weathering. To avoid unrealistically high Ca^{2+} concentrations in surface soil, published values for
334 surface soil Ca^{2+} weathering were used (Aherne et al., 2007) and the error in surface water Ca^{2+} was
335 minimised by adjusting subsoil Ca^{2+} weathering. Parameters governing DOM dynamics were not
336 calibrated separately for the AWMN sites, to determine whether the values established at the
337 experimental sites are applicable more widely. The means of previously fitted values of k_{inpdC} , k_{inpdN}
338 and P_{sites} for peat and podsol were used, and the area proportions of peat and podsol within the lake
339 or stream catchment were used to derive a weighted mean value for the catchment for these
340 parameters.

341

342 The accuracy of simulated data was assessed in relation to observations using the Nash-Sutcliffe
343 coefficient of determination (*NSCD*), calculated as $(1 - \text{residual variance}/\text{variance of measured data})$
344 (Nash and Sutcliffe, 1970). For the AWMN sites, the *NSCD* was calculated using mean observations
345 and mean simulated values for the study period.

346

347 The sensitivity of predicted DOC fluxes to variation in deposition fluxes of S and N, and variation in
348 mean annual temperature and precipitation surplus, was explored for an example site, the control
349 treatment on Migneint podzol. Simulations were carried out using historic and projected deposition
350 fluxes, as above, until 2020. Different rates of S and N deposition, or different combinations of mean
351 annual temperature and precipitation surplus, were then applied and kept constant until 2100. The
352 DOC flux, pH and NPP were assessed in the year following the change (2021) and in 2100.

353

354 The MADOC model was developed to use a relatively small parameter set, for model parsimony and
355 to facilitate upscaling. The MADOC model uses many of the same inputs as VSD, and a regional
356 application to British peat bogs was carried out based on data collated by the UK National Focal
357 Centre for critical loads mapping, as described in Evans et al. (2012a). Spatial data were derived
358 under the Defra Critical Loads and Dynamic Modelling project, <http://cldm.defra.gov.uk/>.

359

360 Results

361

362 Simulated responses of pH and DOC flux corresponded to the measured increases in these quantities
363 in response to acidification and decreases in response to alkalization (Figure 3). Some instability was
364 observed in predicted trajectories of pH and DOC in the alkalised treatments, due to the
365 simplification whereby DOC solubility in the model is determined by pH in the preceding year. This
366 instability was only observed following an abrupt increase in pH. The model predicted DOC fluxes
367 across all measurement years and treatments reasonably well (Figure 4; *NSCD* = 0.61). Values for pH
368 were predicted with less accuracy (Figure 4; *NSCD* = 0.24) but the overall trend of experimental
369 responses was reproduced.

370

371 Model runs for the AWMN surface waters dataset showed reasonable correspondence between
372 MADOC predictions and measured trends in pH and in DOC flux, although there was some
373 inaccuracy in predicted mean values, as illustrated by time-series plots of observations and
374 predictions from an example site (Figure 5). After calibration of Cl deposition rate, Ca weathering
375 rate and the Al equilibrium constant for each site, the MADOC model reproduced measured Cl^- , Al^{3+}
376 and total base cation concentrations (not shown). Without further calibration, values were predicted
377 with limited accuracy for pH (*NSCD* = -0.47, Figure 6a) and better accuracy for DOC flux (*NSCD* = 0.11,
378 Figure 6b). The upward trends in DOC and pH at many sites were reproduced (Figure 6c, 6d),
379 although in most cases the model over-predicted increases in pH, and under-predicted increases in
380 DOC.

381

382 Responses of the model to different N and S deposition rates applied from 2020 are shown in Figure
383 7. Soil solution pH responded as expected, showing an effect of S in the year immediately following
384 application of the new loading. Initially, N loading did not affect pH, since all of the applied N was
385 either immobilised or taken up by plants, and was therefore not leached. After 80 years, greater N
386 deposition rates gave rise to N-saturation, more N leaching, and somewhat lower pH. The DOC flux
387 initially responded only to changes in S deposition, with more S giving lower pH and decreased DOC
388 flux. However, after 80 years the effects of N deposition are also evident, and the cumulative effects
389 of N on net primary productivity (NPP) and therefore the release of DOC from relatively young
390 organic material led to greater DOC fluxes at higher N loadings.

391

392 Responses of the model to changes in precipitation surplus and mean annual temperature, applied
393 from 2020-2100, showed only minor differences in initial response and response after 80 years
394 (Figure 8). There was a clear increase in NPP with mean annual temperature, but little effect of
395 precipitation surplus on NPP. The DOC flux increased with temperature, principally as a result of
396 greater NPP at higher temperatures, and also increased with precipitation surplus, since a greater

397 volume of soil water increased the amount of PDOC in the solute phase. The pH response to climatic
398 changes was driven by simulated DOC flux, with greater DOC fluxes resulting in lower pH values.
399

400 The example maps (Figure 9) illustrate the spatial variation in pH and DOC across UK peat bogs, as
401 simulated by the MADOC model. Larger DOC fluxes were simulated in peat towards the south and
402 east than in the north and west, and coincided with lower simulated pH. Areas with low pH and large
403 DOC fluxes were associated with large rates of N and also S deposition. A simple interpretation that
404 DOC flux is controlled within the model by productivity stimulation rather than by acid suppression
405 would be incorrect, however, since areas with high current S deposition also historically received
406 very large S inputs and have therefore recovered from acidification more strongly. The simulations
407 suggest that the spatial pattern of DOC in the UK is determined by both pH increase with reductions
408 in S deposition, and by productivity stimulation by ongoing N pollution.
409

410 Discussion

411
412 Increases in pH and DOC in alkalisated experimental treatments, and decreases in acidified treatments,
413 were reproduced by the MADOC model. The changes were largely due to increased solubilisation of
414 PDOC as a result of higher pH, reflecting observations in field studies which have attributed DOC
415 increase to recovery from acidification (Haaland et al., 2010; Monteith et al., 2007; SanClements et
416 al., 2012). The buffering effect of DOC on pH was well represented. The model also reproduced
417 changes in pH and DOC in the independent dataset from the AWMN with minimal extra calibration.
418 In contrast to the soil solution sampled in the experimental treatments, the AWMN samples were
419 obtained from stream and lake samples, and hence many had greater pH and base cation
420 concentrations due to the influence of basal flow paths through deeper mineral soil. By calibrating
421 the aluminium equilibrium constant and base cation weathering rates, stream and lake base cation
422 concentrations were successfully reproduced. Without further calibration, the predicted pH and DOC
423 fluxes for the independent dataset matched observations reasonably well (Figure 6). Further
424 calibration could be used to increase accuracy – for example, fitting site-specific values for k_{inpdC}
425 resulted in considerable improvements in prediction accuracy for pH ($NSCD = 0.01$) and DOC flux
426 ($NSCD = 0.64$) (data not shown). These results give some confidence that the MADOC model can
427 simulate DOC and pH change in a range of environments.
428

429 The observed lack of pH response to experimental acid and alkali additions on the Migneint peat site
430 (Figure 3a) was not simulated by the model, and was the main cause of inaccuracy in overall
431 performance (Figure 4a). This lack of response may have been due to the dilution of treatments by
432 lateral water movement at this very wet site, where water tables frequently come close to the
433 surface, above the zone in which soil solution samplers were located. This interpretation is
434 supported by small observed changes in Na^+ concentrations in the alkaline (NaOH) addition
435 treatments on this site (data not shown). On this basis, we conclude that poor performance of the
436 model at this site was at least partially explained by issues relating to the experimental site itself.
437

438 When applied at catchment scale the model performed less well, in particular overestimating the
439 rate of pH change and underestimating the rate of DOC change over the approximately 20 year
440 period. This suggests that the simulations should have included a greater effect of pH increase on
441 DOC dissolution from mineral soil layers, which would have buffered the simulated pH increase.
442 Complexation of DOC with aluminium in the mineral soil at lower pH, which was not simulated, may
443 also partially explain the greater apparent sensitivity of DOC concentrations in surface waters to
444 changes in sulphur deposition, compared to those surface organic soil horizons, and thus the larger
445 observed versus modelled rate of increase of surface water DOC with recovery from acidification
446 (Evans et al., 2012b).
447

448 Simulated DOC fluxes proved sensitive to several factors that have been highlighted by previous
449 authors, notably soil solution pH, but were also strongly affected by plant productivity and the
450 resultant increase in soil organic matter in the fast-turnover pool. The main processes governing
451 DOC concentration within the model are illustrated by sensitivity plots (Figure 7, Figure 8). In the
452 year following a change in simulated N and S load, effects on DOC flux are dominated by pH change
453 on the solubility of the pre-existing PDOM pool, and hence DOC flux is correlated with changes to
454 the S load rather than to the N load. However, after maintaining simulated application rates for 80
455 years, changes in simulated DOC flux were also strongly affected by the effects of N deposition on
456 plant productivity. The DOC flux is simulated as a constant proportion of total organic matter
457 decomposition, most of which is of the active organic matter pool that is derived from plant
458 production in the previous year. This matches observations that much DOC is of recent origin (Evans
459 et al., 2007; Raymond et al., 2007; Tipping et al., 2010).

460
461 The simulated productivity increase due to release from N limitation is realistic, although whether
462 this increase will be sustained is questionable. Limitation by N is widespread (LeBauer and Treseder,
463 2008) and so an initial increase in productivity with more N deposition is likely. Other limitations to
464 plant growth may then start to dominate, such as temperature, drought, water saturation or
465 deficiencies in other nutrients (Braun et al., 2010). Nitrogen can be obtained from the atmosphere,
466 so the supply of phosphorus and other elements obtained from mineral weathering may be a more
467 fundamental long-term constraint (Menge et al., 2012). However, increased N availability can
468 increase the supply of other plant nutrients (Olander and Vitousek, 2000; Rowe et al., 2008) leading
469 to eventual nutrient element co-limitation in many ecosystems (Elser et al., 2007; Vitousek et al.,
470 2010). In a review of the effects on DOC fluxes of experimental N additions, Evans et al. (2008a)
471 concluded that direct effects of N on plant growth and organic matter cycling were often obscured
472 by pH changes resulting from the ionic form of the N applied and counter-ion additions. In a gradient
473 study, (Bragazza et al., 2006) concluded that DOC concentrations increased with N deposition, noting
474 that N deposition can increase enzyme fluxes, increase plant productivity, and drive changes in plant
475 species composition towards more easily-decomposed species. The predicted increase in DOC flux
476 with N deposition corresponds to this trend, and suggests that effects of recovery from acidification
477 on DOC solubility may not be acting in isolation, but rather are reinforcing a more gradual long-term
478 increase in DOC linked to rising productivity. Further research is needed to test this hypothesis.

479
480 Oulehle et al. (in press) proposed a switch in determination of DOC fluxes from 'solubility control' to
481 'supply control'. Supply control implies that a change in pH and therefore DOC solubility will change
482 the PDOC pool, eventually causing DOC fluxes to become more similar to fluxes before the pH
483 change. Increased pH will increase PDOC dissolution, depleting the PDOC pool, whereas decreased
484 pH will allow a larger PDOC pool to build up and eventually increase DOC fluxes again. However,
485 retained PDOC is susceptible to mineralisation, so DOC fluxes are unlikely to revert entirely to values
486 observed before the pH change. In the simulations presented, changes to DOC fluxes due to
487 acidification or alkalinisation were maintained, with only a small tendency for concentrations to revert
488 towards the values in the control treatment. A given increase in DOC flux may be explained equally
489 well by a PDOC pool that turns over slowly or rapidly, although these alternatives affect the speed
490 and extent with which the DOC flux returns to its previous value following a change in pH (Figure
491 10). A PDOC pool with a large turnover rate results in more sustained increase in DOC as a result of
492 pH increase, whereas if input and output PDOC fluxes are smaller, the rise is more short-lived. The
493 experimental dataset has not run for long enough to distinguish these effects, and we are uncertain
494 as to which type of response prevails. Increases in DOC with recovery from acidification seem likely
495 to have been sustained, given that they are noticeable in long-term monitoring datasets and across
496 sites with distinct deposition histories (Evans et al., 2005). However, many of these observations
497 have taken place against a background of continuously declining S deposition, so it is not certain that
498 concentrations will remain high once S inputs have stabilised.

499

500 The predicted increase in DOC flux with precipitation surplus (Figure 8) corresponded to
501 observations that DOC flux is correlated with water flux (Buckingham et al., 2008) and that DOC
502 concentrations are less strongly reduced by precipitation than would be suggested by a simple
503 dilution model (Haaland et al., 2008; van den Berg et al., 2012). Although the increase in simulated
504 DOC flux was not proportionate to the increase in precipitation surplus, greater volumes of water
505 increased the partitioning of PDOC into the dissolved phase. Simulated DOC fluxes increased with
506 temperature, mainly because higher temperatures stimulated organic matter turnover and N
507 mineralisation. This effect seems likely to be masked by continuing N pollution in many ecosystems.

508

509 The simulated effects and interactions may be formulated as hypotheses generated by the model:

510 **H1:** Spatial and/or temporal patterns of DOC increase are related to patterns of plant productivity
511 increase as well as to recovery from acidification.

512 **H2:** The cumulative effects of fertilisation by reactive N deposition, and reduced mineralisation of
513 PDOC resulting from more rapid solubilisation and leaching, will cause a sustained increase in
514 DOC even after soil pH has stabilised.

515 These hypotheses could be tested against survey and long-term monitoring datasets, although
516 controlled field or lab experiments may be necessary to separate the effects of N and S pollution.

517

518 Predictive representations of DOC dynamics are essential for closing C budgets in ecosystem models
519 and understanding interactions between pollutant deposition, changes in C stock, water quality and
520 climate change. Despite the existence of significant feedbacks between pH and DOC flux, and
521 between NPP and N flux, a relatively simple integrated model proved capable of reproducing the
522 effects of key drivers as observed in experiments and surveys. The study illustrates the value of
523 constraining the overall complexity and parameter requirement of an integrated model by using
524 simple components. As well as predicting changes to DOC and pH, the MADOC model can be used to
525 explore the effects of multiple pollutant and climate drivers on multiple endpoints including soil
526 total C and N, plant-available N, plant productivity and nitrate leaching, and so will be useful for
527 analysing a range of policy scenarios.

528

529 **Acknowledgements**

530

531 The development of the MADOC model was funded by the Department for Environment, Food and
532 Rural Affairs of the UK under the project "Critical loads and dynamic modelling for acidity and
533 nitrogen" <http://cldm.defra.gov.uk/>, by the European Union under the ECLAIRE project, and by the
534 Natural Environment Research Council under the EHFI project. We are grateful to Rachel Helliwell of
535 the James Hutton Institute for providing AWMN data.

536

537 **References**

538

539 Aherne, J., Helliwell, R.C., Lilly, A., Ferrier, R.C., Jenkins, A., 2007. Simulation of soil and surface water
540 acidification: Divergence between one-box and two-box models? *Applied Geochemistry* 22, 1167-
541 1173.

542 Aitkenhead-Peterson, J.A., Alexander, J.E., Clair, T.A., 2005. Dissolved organic carbon and dissolved
543 organic nitrogen export from forested watersheds in Nova Scotia: Identifying controlling factors.
544 *Global Biogeochemical Cycles* 19.

545 Aitkenhead-Peterson, J.A., McDowell, W.H., Neff, J.C., 2003. Sources, production, and regulation of
546 allochthonous dissolved organic matter inputs to surface waters., in: Findlay, S., Sinsabaugh, R.L.
547 (Eds.), *Aquatic ecosystems : interactivity of dissolved organic matter.*, pp. 25-59.

548 Billett, M.F., Dinsmore, K.J., Smart, R.P., Garnett, M.H., Holden, J., Chapman, P., Baird, A.J., Grayson,
549 R., Stott, A.W., 2012. Variable source and age of different forms of carbon released from natural
550 peatland pipes. *Journal of Geophysical Research-Biogeosciences* 117.

551 Bontemps, J.D., Herve, J.C., Leban, J.M., Dhote, J.F., 2011. Nitrogen footprint in a long-term
552 observation of forest growth over the twentieth century. *Trees-Structure and Function* 25, 237-
553 251.

554 Borken, W., Ahrens, B., Schulz, C., Zimmermann, L., 2011. Site-to-site variability and temporal trends
555 of DOC concentrations and fluxes in temperate forest soils. *Global Change Biology* 17, 2428-2443.

556 Bragazza, L., Freeman, C., Jones, T., Rydin, H., Limpens, J., Fenner, N., Ellis, T., Gerdol, R., Hajek, M.,
557 Hajek, T., Lacumin, P., Kutnar, L., Tahvanainen, T., Toberman, H., 2006. Atmospheric nitrogen
558 deposition promotes carbon loss from peat bogs. *Proceedings of the National Academy of
559 Sciences of the United States of America* 103, 19386-19389.

560 Braun, S., Thomas, V.F.D., Quiring, R., Fluckiger, W., 2010. Does nitrogen deposition increase forest
561 production? The role of phosphorus. *Environmental Pollution* 158, 2043-2052.

562 Buckingham, S., Tipping, E., Hamilton-Taylor, J., 2008. Concentrations and fluxes of dissolved organic
563 carbon in UK topsoils. *Science of the Total Environment* 407, 460-470.

564 Buffam, I., Galloway, J.N., Blum, L.K., McGlathery, K.J., 2001. A stormflow/baseflow comparison of
565 dissolved organic matter concentrations and bioavailability in an Appalachian stream.
566 *Biogeochemistry* 53, 269-306.

567 Chow, A.T., Tanji, K.K., Gao, S.D., 2003. Production of dissolved organic carbon (DOC) and
568 trihalomethane (THM) precursor from peat soils. *Water Research* 37, 4475-4485.

569 Clark, J.M., Bottrell, S.H., Evans, C.D., Monteith, D.T., Bartlett, R., Rose, R., Newton, R.J., Chapman,
570 P.J., 2010. The importance of the relationship between scale and process in understanding long-
571 term DOC dynamics. *Science of the Total Environment* 208, 2768-2775.

572 Clutterbuck, B., Yallop, A.R., 2010. Land management as a factor controlling dissolved organic carbon
573 release from upland peat soils: 2. Changes in DOC productivity over four decades. *Science of the
574 Total Environment* 408, 6179-6191.

575 De Wit, H.A., Mulder, J., Hindar, A., Hole, L., 2007. Long-term increase in dissolved organic carbon in
576 streamwaters in Norway is response to reduced acid deposition. *Environmental Science &
577 Technology* 41, 7706-7713.

578 DeForest, J.L., Zak, D.R., Pregitzer, K.S., Burton, A.J., 2004. Atmospheric nitrate deposition and the
579 microbial degradation of cellobiose and vanillin in a northern hardwood forest. *Soil Biology &
580 Biochemistry* 36, 965-971.

581 DeForest, J.L., Zak, D.R., Pregitzer, K.S., Burton, A.J., 2005. Atmospheric nitrate deposition and
582 enhanced dissolved organic carbon leaching: Test of a potential mechanism. *Soil Science Society
583 of America journal* 69, 1233-1237.

584 Dore, A., Kryza, M., Hallsworth, S., Matejko, M., Vieno, M., Hall, J., Van Oijen, M., Zhang, Y., Smith,
585 R., Sutton, M.A., 2009. Modelling the deposition and concentration of long range air pollutants.
586 Final report on DEFRA contract CO3021. Centre for Ecology and Hydrology, Edinburgh., p. 65.

587 Elser, J.J., Bracken, M.E.S., Cleland, E.E., Gruner, D.S., Harpole, W.S., Hillebrand, H., Ngai, J.T.,
588 Seabloom, E.W., Shurin, J.B., Smith, J.E., 2007. Global analysis of nitrogen and phosphorus
589 limitation of primary producers in freshwater, marine and terrestrial ecosystems. *Ecology Letters*
590 10, 1135-1142.

591 Emmett, B.A., Reynolds, B., Silgram, M., Sparks, T.H., Woods, C., 1998. The consequences of chronic
592 nitrogen additions on N cycling and soilwater chemistry in a Sitka spruce stand, North Wales.
593 *Forest Ecology and Management* 101, 165-175.

594 Evans, C., Hall, J., Rowe, E., Tipping, E., Helliwell, R., Smart, S., Norris, D., Cooper, D., Coull, M.,
595 Moldan, F., Blomgren, H., McDougall, G., Aherne, J., Oulehle, F., Cosby, J., Hutchins, M., Woods,
596 C., Lawlor, A., Jenkins, A., 2010a. Critical Loads and Dynamic Modelling Umbrella: Final Report for
597 the period 2007 to 2010. Report to Defra under contract AQ801 Critical Loads and Dynamic
598 Modelling. NERC/Centre for Ecology & Hydrology. 132 pp.

599 Evans, C., Hall, J., Rowe, E., Tipping, E., Henrys, P., Smart, S., Moldan, F., Blomgren, H., Oulehle, F.,
600 Norris, D., Helliwell, R., Cosby, J., Jenkins, A., 2012a. Critical Loads and Dynamic Modelling
601 Umbrella - Draft Final Report on the contract extension April 2010 to September 2011 and
602 extension to April 2012. Centre for Ecology and Hydrology project NEC03418. Report to Defra
603 under contract AQ0801.

604 Evans, C.D., Chapman, P.J., Clark, J.M., Monteith, D.T., Cresser, M.S., 2006. Alternative explanations
605 for rising dissolved organic carbon export from organic soils. *Global Change Biology* 12, 2044-
606 2053.

607 Evans, C.D., Cooper, D.M., Monteith, D.T., Helliwell, R.C., Moldan, F., Hall, J., Rowe, E.C., Cosby, B.J.,
608 2010b. Linking monitoring and modelling: can long-term datasets be used more effectively as a
609 basis for large-scale prediction? *Biogeochemistry* 101, 211-227.

610 Evans, C.D., Freeman, C., Cork, L.G., Thomas, D.N., Reynolds, B., Billett, M.F., Garnett, M.H., Norris,
611 D., 2007. Evidence against recent climate-induced destabilisation of soil carbon from C-14
612 analysis of riverine dissolved organic matter. *Geophysical Research Letters* 34.

613 Evans, C.D., Goodale, C.L., Caporn, S.J.M., Dise, N.B., Emmett, B.A., Fernandez, I.J., Field, C.D.,
614 Findlay, S.E.G., Lovett, G.M., Meesenburg, H., Moldan, F., Sheppard, L.J., 2008a. Does elevated
615 nitrogen deposition or ecosystem recovery from acidification drive increased dissolved organic
616 carbon loss from upland soil? A review of evidence from field nitrogen addition experiments.
617 *Biogeochemistry* 91, 13-35.

618 Evans, C.D., Helliwell, R.C., Coull, M.C., Langan, S.J., Hall, J., 2004. Results of a survey of UK soils to
619 provide input data for national-scale dynamic modelling. Report to DEFRA, contract CPEA19.
620 Centre for Ecology and Hydrology, Bangor, UK.

621 Evans, C.D., Jones, T.G., Burden, A., Ostle, N., Zieliński, P., Cooper, M.D.A., Peacock, M., Clark, J.M.,
622 Oulehle, F., Cooper, D., Freeman, C., 2012b. Acidity controls on dissolved organic carbon mobility
623 in organic soils. *Global Change Biology* 18, 3317-3331.

624 Evans, C.D., Monteith, D.T., Cooper, D.M., 2005. Long-term increases in surface water dissolved
625 organic carbon: Observations, possible causes and environmental impacts. *Environmental*
626 *Pollution* 137, 55-71.

627 Evans, C.D., Monteith, D.T., Reynolds, B., Clark, J.M., 2008b. Buffering of recovery from acidification
628 by organic acids. *Science of the Total Environment* 404, 316-325.

629 Fernandez, I.J., Rustad, L.E., 1990. Soil response to S and N treatments in a northern New-England
630 low elevation coniferous forest. *Water Air and Soil Pollution* 52, 23-39.

631 Filep, T., Rekası, M., 2011. Factors controlling dissolved organic carbon (DOC), dissolved organic
632 nitrogen (DON) and DOC/DON ratio in arable soils based on a dataset from Hungary. *Geoderma*
633 162, 312-318.

634 Findlay, S.E.G., 2005. Increased carbon transport in the Hudson River: unexpected consequence of
635 nitrogen deposition? *Frontiers in Ecology and the Environment* 3, 133-137.

636 Freeman, C., Evans, C.D., Monteith, D.T., Reynolds, B., Fenner, N., 2001. Export of organic carbon
637 from peat soils. *Nature* 412, 785.

638 Futter, M.N., Butterfield, D., Cosby, B.J., Dillon, P.J., Wade, A.J., Whitehead, P.G., 2007. Modeling the
639 mechanisms that control in-stream dissolved organic carbon dynamics in upland and forested
640 catchments. *Water Resources Research* 43.

641 Haaland, S., Austnes, K., Kaste, O., Mulder, J., Riise, G., Vestgarden, L.S., Stuanes, A.O., 2008.
642 Manipulation of precipitation in small headwater catchments at Storgama, Norway: Effects on
643 leaching of organic carbon and nitrogen species. *Ambio* 37, 48-55.

644 Haaland, S., Hongve, D., Laudon, H., Riise, G., Vogt, R.D., 2010. Quantifying the drivers of the
645 increasing colored organic matter in boreal surface waters. *Environmental Science & Technology*
646 44, 2975-2980.

647 Hagedorn, F., Schleppe, P., Waldner, P., Fluhler, H., 2000. Export of dissolved organic carbon and
648 nitrogen from Gleysol dominated catchments - the significance of water flow paths.
649 *Biogeochemistry* 50, 137-161.

650 Hall, J., Ulliyett, J., Heywood, L., Broughton, R., Fawehinmi, J., 2003. Status of UK Critical Loads:
651 Critical Loads methods, data and maps. Centre for Ecology and Hydrology, Monks Wood. Report to
652 DEFRA (Contract EPG 1/3/185). p. 77.

653 Harrison, A.F., Taylor, K., Scott, A., Poskitt, J., Benham, D., Grace, J., Chaplow, J., Rowland, P., 2008.
654 Potential effects of climate change on DOC release from three different soil types on the
655 Northern Pennines UK: examination using field manipulation experiments. *Global Change Biology*
656 14, 687-702.

657 Hogberg, P., Fan, H.B., Quist, M., Binkley, D., Tamm, C.O., 2006. Tree growth and soil acidification in
658 response to 30 years of experimental nitrogen loading on boreal forest. *Global Change Biology*
659 12, 489-499.

660 Holden, J., Chapman, P.J., Palmer, S.M., Kay, P., Grayson, R., 2012. The impacts of prescribed
661 moorland burning on water colour and dissolved organic carbon: A critical synthesis. *Journal of*
662 *Environmental Management* 101, 92-103.

663 Hongve, D., Riise, G., Kristiansen, J.F., 2004. Increased colour and organic acid concentrations in
664 Norwegian forest lakes and drinking water - a result of increased precipitation? *Aquatic Sciences*
665 66, 231-238.

666 Jutras, M.F., Nasr, M., Castonguay, M., Pit, C., Pomeroy, J.H., Smith, T.P., Zhang, C.F., Ritchie, C.D.,
667 Meng, F.R., Clair, T.A., Arp, P.A., 2011. Dissolved organic carbon concentrations and fluxes in
668 forest catchments and streams: DOC-3 model. *Ecological Modelling* 222, 2291-2313.

669 Kalbitz, K., Solinger, S., Park, J.H., Michalzik, B., Matzner, E., 2000. Controls on the dynamics of
670 dissolved organic matter in soils: A review. *Soil Science* 165, 277-304.

671 Kerkhoff, A.J., Enquist, B.J., Elser, J.J., Fagan, W.F., 2005. Plant allometry, stoichiometry and the
672 temperature-dependence of primary productivity. *Global Ecology and Biogeography* 14, 585-598.

673 Krug, E.C., Frink, C.R., 1983. Acid-rain on acid soil: a new perspective. *Science* 221, 520-525.

674 Larsen, S., Andersen, T., Hessen, D.O., 2011a. Climate change predicted to cause severe increase of
675 organic carbon in lakes. *Global Change Biology* 17, 1186-1192.

676 Larsen, S., Andersen, T., Hessen, D.O., 2011b. Predicting organic carbon in lakes from climate drivers
677 and catchment properties. *Global Biogeochemical Cycles* 25: doi: 10.1029/2010gb003908

678 Laudon, H., Berggren, M., Agren, A., Buffam, I., Bishop, K., Grabs, T., Jansson, M., Kohler, S., 2011.
679 Patterns and dynamics of dissolved organic carbon (DOC) in boreal streams: the role of processes,
680 connectivity, and scaling. *Ecosystems* 14, 880-893.

681 LeBauer, D.S., Treseder, K.K., 2008. Nitrogen limitation of net primary productivity in terrestrial
682 ecosystems is globally distributed. *Ecology* 89, 371-379.

683 Ledesma, J.L.J., Kohler, S.J., Futter, M.N., 2012. Long-term dynamics of dissolved organic carbon:
684 Implications for drinking water supply. *Science of the Total Environment* 432, 1-11.

685 Lu, C.Q., Tian, H.Q., Liu, M.L., Ren, W., Xu, X.F., Chen, G.S., Zhang, C., 2012. Effect of nitrogen
686 deposition on China's terrestrial carbon uptake in the context of multifactor environmental
687 changes. *Ecological Applications* 22, 53-75.

688 Menge, D.N.L., Hedin, L.O., Pacala, S.W., 2012. Nitrogen and phosphorus limitation over long-term
689 ecosystem development in terrestrial ecosystems. *PLoS ONE* 7.

690 Michalzik, B., Tipping, E., Mulder, J., Lancho, J.F.G., Matzner, E., Bryant, C.L., Clarke, N., Lofts, S.,
691 Esteban, M.A.V., 2003. Modelling the production and transport of dissolved organic carbon in
692 forest soils. *Biogeochemistry* 66, 241-264.

693 Monteith, D.T., Evans, C.D., 2005. The United Kingdom Acid Waters Monitoring Network: a review of
694 the first 15 years and introduction to the special issue. *Environmental Pollution* 137, 3-13.

695 Monteith, D.T., Shilland, E.M., 2007. The United Kingdom Acid Waters Monitoring Network:
696 Assessment of the first 18 years of data. Data summary annex accompanying research project
697 final report. Report to Defra (contract EPG 1/3/160). ENSIS Ltd., London.

698 Monteith, D.T., Stoddard, J.L., Evans, C.D., de Wit, H.A., Forsius, M., Hogasen, T., Wilander, A.,
699 Skjelkvale, B.L., Jeffries, D.S., Vuorenmaa, J., Keller, B., Kopacek, J., Vesely, J., 2007. Dissolved

700 organic carbon trends resulting from changes in atmospheric deposition chemistry. *Nature* 450,
701 537-U539.

702 Nash, J.E., Sutcliffe, J.V., 1970. River flow forecasting through conceptual models part I — A
703 discussion of principles. *Journal of Hydrology* 10, 282–290.

704 Neff, J.C., Asner, G.P., 2001. Dissolved organic carbon in terrestrial ecosystems: Synthesis and a
705 model. *Ecosystems* 4, 29-48.

706 Nelder, J.A., Mead, R., 1965. A simplex method for function minimization. *Computer Journal* 7, 308-
707 313.

708 Olander, L.P., Vitousek, P.M., 2000. Regulation of soil phosphatase and chitinase activity by N and P
709 availability. *Biogeochemistry* 49, 175-190.

710 Oulehle, F., Hruska, J., 2009. Rising trends of dissolved organic matter in drinking-water reservoirs as
711 a result of recovery from acidification in the Ore Mts., Czech Republic. *Environmental Pollution*
712 157, 3433-3439.

713 Oulehle, F., Jones, T.G., Evans, C.D., Tipping, E., Burden, A., Cooper, M.D.A., Robinson, I., Zielinski, P.,
714 in press. Soil-solution partitioning of DOC in acid organic soils: Results from a field acidification
715 and alkalization experiment. *European Journal of Soil Science*.

716 Patrick, S., Waters, D., Juggins, S., Jenkins, A., 1991. The United Kingdom Acid Waters Monitoring
717 Network: site descriptions and methodology report. Report to Dept of the Environment and Dept
718 of the Environment (Northern Ireland). ENSIS Ltd., London. ISBN 1 871275 04 0.

719 Posch, M., Reinds, G.J., 2009. A very simple dynamic soil acidification model for scenario analyses
720 and target load calculations. *Environmental Modelling & Software* 24, 329-340.

721 Pregitzer, K.S., Zak, D.R., Burton, A.J., Ashby, J.A., MacDonald, N.W., 2004. Chronic nitrate additions
722 dramatically increase the export of carbon and nitrogen from northern hardwood ecosystems.
723 *Biogeochemistry* 68, 179-197.

724 Raymond, P.A., McClelland, J.W., Holmes, R.M., Zhulidov, A.V., Mull, K., Peterson, B.J., Striegl, R.G.,
725 Aiken, G.R., Gurtovaya, T.Y., 2007. Flux and age of dissolved organic carbon exported to the Arctic
726 Ocean: A carbon isotopic study of the five largest arctic rivers. *Global Biogeochemical Cycles* 21.

727 Rowe, E.C., Smart, S.M., Kennedy, V.H., Emmett, B.A., Evans, C.D., 2008. Nitrogen deposition
728 increases the acquisition of phosphorus and potassium by heather *Calluna vulgaris*.
729 *Environmental Pollution* 155, 201-207.

730 SanClements, M.D., Oelsner, G.P., McKnight, D.M., Stoddard, J.L., Nelson, S.J., 2012. New insights
731 into the source of decadal increases of dissolved organic matter in acid-sensitive lakes of the
732 northeastern United States. *Environmental Science & Technology* 46, 3212-3219.

733 Sleutel, S., Vandenbruwane, J., De Schrijver, A., Wuyts, K., Moeskops, B., Verheyen, K., De Neve, S.,
734 2009. Patterns of dissolved organic carbon and nitrogen fluxes in deciduous and coniferous
735 forests under historic high nitrogen deposition. *Biogeosciences* 6, 2743-2758.

736 Smith, R.I., Fowler, D., Sutton, M.A., Flechard, C., Coyle, M., 2000. Regional estimation of pollutant
737 gas deposition in the UK: model description, sensitivity analyses and outputs. *Atmospheric*
738 *Environment* 34, 3757-3777.

739 Stuanes, A.O., Kjonaas, O.J., 1998. Soil solution chemistry during four years of NH₄NO₃ addition to a
740 forested catchment at Gardsjon, Sweden. *Forest Ecology and Management* 101, 215-226.

741 Tipping, E., 1990. Interactions of organic acids with inorganic and organic surfaces., in: Perdue, E.M.,
742 Gjessing, E.T. (Eds.), *Organic acids in aquatic ecosystems*. John Wiley & Sons, Chichester., pp. 209-
743 221.

744 Tipping, E., Billett, M.F., Bryant, C.L., Buckingham, S., Thacker, S.A., 2010. Sources and ages of
745 dissolved organic matter in peatland streams: evidence from chemistry mixture modelling and
746 radiocarbon data. *Biogeochemistry* 100, 121-137.

747 Tipping, E., Rowe, E.C., Evans, C.D., Mills, R.T.E., Emmett, B.A., Chaplow, J.S., Hall, J.R., 2012. N14C: a
748 plant-soil nitrogen and carbon cycling model to simulate terrestrial ecosystem responses to
749 atmospheric nitrogen deposition. *Ecological Modelling* 247, 11-26.

750 UBA, 2004. Manual on methodologies and criteria for modelling and mapping critical loads & levels
751 and air pollution effects, risks and trends. Umwelt Bundes Amt (Federal Environment Agency),
752 Berlin., p. 235.

753 van den Berg, L.J.L., Shotbolt, L., Ashmore, M.R., 2012. Dissolved organic carbon (DOC)
754 concentrations in UK soils and the influence of soil, vegetation type and seasonality. *Science of
755 the Total Environment* 427, 269-276.

756 Vitousek, P.M., Howarth, R.W., 1991. Nitrogen limitation on land and in the sea - How can it occur?
757 *Biogeochemistry* 13, 87-115.

758 Vitousek, P.M., Porder, S., Houlton, B.Z., Chadwick, O.A., 2010. Terrestrial phosphorus limitation:
759 mechanisms, implications, and nitrogen-phosphorus interactions. *Ecological Applications* 20, 5-
760 15.

761 Wei, X.H., Blanco, J.A., Jiang, H., Kimmins, J.P.H., 2012. Effects of nitrogen deposition on carbon
762 sequestration in Chinese fir forest ecosystems. *Science of the Total Environment* 416, 351-361.

763 Xu, N., Saiers, J.E., Wilson, H.F., Raymond, P.A., 2012. Simulating streamflow and dissolved organic
764 matter export from a forested watershed. *Water Resources Research* 48, W05519,
765 doi:10.1029/2011wr011423, 18.

766

767

768
769
770
771

Tables

Table 1. Fixed input values for the MADOC model.

Parameter	Description	Value
k_{minpd}	Proportion of potential DOC mineralised, yr^{-1}	0.432 ^a
α_{org}	DOC sorption constant in organic soil, $\text{m}^3 \text{g}^{-1} \text{L mol}^{-1}$	2.20×10^6 ^a
α_{min}	DOC sorption constant in mineral soil, $\text{m}^3 \text{g}^{-1} \text{L mol}^{-1}$	7.62×10^6 ^a
$pKpar(1)$	1 st dissociation constant for triprotic organic acids	3.5 ^b
$pKpar(2)$	2 nd dissociation constant for triprotic organic acids	4.4 ^b
$pKpar(3)$	3 rd dissociation constant for triprotic organic acids	5.5 ^b
K_{HBc}	selectivity constant for H-Bc exchange	199.5 ^c
exp_{Al}	aluminium equilibrium exponent	1.85 ^d
k_{inpdN}	Proportion of N turnover entering potentially-dissolved pool	0.0274 ^a

772 ^a fitted; ^b (Oulehle et al., in press); ^c (Hall et al., 2003); ^d (UBA, 2004).
773

774
775
776
777
778

Table 2. Site-specific inputs for the MADOC model. Values used for the experimental sites: Migneint peat (MPT); Migneint podzol (MPZ); Peak District peat (PPT) and Peak District podzol (PPZ), and the ranges of values used for Acid Waters Monitoring Network sites (AWMN) and for UK peat bog (UK peat) are shown.

Input	Description	MPT	MPZ	PPT	PPZ	AWMN	UK peat
K_{AlOx}	aluminium equilibrium constant	0.059 ^a	0.295 ^a	0.531 ^a	0.567 ^a	0.16 – 54.5 ^a	0.295 ^b
k_{inpdC}	Proportion of C turnover entering potentially-dissolved pool	0.347 ^a	0.493 ^a	0.825 ^a	0.472 ^a	0.534 ^c	0.586 ^b
P_{sites}	Dissociable protons per mol DOC, eq(-) mol ⁻¹	0.080 ^a	0.076 ^a	0.191 ^a	0.118 ^a	0.116 ^c	0.136 ^b
P_{Bby}	Proportion of leachate from topsoil that does not interact with subsoil	1	0	1	0	0.07 – 0.60 ^d	1
W_{Na}	weathering rate for Na, meq m ⁻³ yr ⁻¹	89 ^a	20 ^a	604 ^a	0.2 ^a	1.8 – 182 ^e	1.8 ^e
W_{Ca}	topsoil weathering rate for Ca meq m ⁻³ yr ⁻¹	264 ^a	786 ^a	271 ^a	202 ^a	127 – 383 ^f	268 ^b
W_{CaSub}	subsoil weathering rate for Ca meq m ⁻² yr ⁻¹	-	-	-	-	0 – 297 ^a	-
T_{org}	thickness of organic soil horizon, m	0.1 ^g	0.1 ^g	0.1 ^g	0.1 ^g	0.02 – 0.35 ^h	0.5
T_{min}	thickness of mineral soil horizon, m	0 ^g	0 ^g	0 ^g	0 ^g	0 – 0.29 ^h	0
$PPTN$	annual precipitation, m	2.20 ⁱ	2.20 ⁱ	1.20 ⁱ	1.20 ⁱ	852 – 3820 ^h	548-3792 ⁱ
W_d	precipitation surplus or drainage flux, m yr ⁻¹	1.99 ^j	1.99 ^j	0.95 ^j	0.95 ^j	0.40 – 3.47 ^h	0.12-3.62 ^j
BD	soil field bulk density, kg dry mass L ⁻¹	0.08 ^e	0.34 ^e	0.16 ^e	0.23 ^e	0.19 – 1.22 ^h	0.16-0.22 ^e
θ	average annual volumetric water content, m ³ m ⁻³	0.91 ^e	0.66 ^e	0.86 ^e	0.71 ^e	0.78 ^c	0.88 ^e
P_{nit}	nitrate proportion of (nitrate + ammonium)	0.22 ^e	0.73 ^e	0.16 ^e	0.66 ^e	0.07 – 0.93 ^h	0.19 ^e
MAT	mean annual temperature, °C	8.1 ^e	8.1 ^e	7.8 ^e	7.8 ^e	3.3 – 10.0 ^h	7.2 ^k
$Planttype$	1=Broadleaf, 2=Conifer,3=Herbs,4=Shrub	4	4	4	4	2 – 4 ^h	4
CEC	cation exchange capacity, meq kg ⁻¹	621 ^j	83 ^j	621 ^j	83 ^j	154 – 997 ^h	621 ^e
f_{Sret}	proportion of S deposition retained	0.49 ^a	0 ^a	0 ^a	0 ^a	0	0.69 ^e
K_{AlBc}	selectivity constant for Al-Bc exchange	8.7 ^j	6.3 ^j	8.7 ^j	6.3 ^j	7.5 ^c	8.7 ^e

779 ^a fitted; ^b mean of values fitted for experimental peat sites; ^c mean of values fitted for all
780 experimental sites; ^d mean weighted by areas of soil types in catchments, Rachel Helliwell *pers.*
781 *com.*; ^e UK NFC values, based on soil and vegetation type (Evans et al., 2004); ^f (Aherne et al., 2007); ^g
782 (Evans et al., 2010a); ^h (Monteith and Shilland, 2007); ⁱ Standard-period Average Annual Rainfall
783 1961-1990 (SAAR6190) provided by UK Met Office; ^j (Hall et al., 2003); ^k mean of AWMN sites.

784
785

786
787
788
789

Figure captions

790 **Figure 1. Model of Acidity Dynamics and Organic Carbon (MADOC): structure in terms of component models**
791 **(N14C, VSD and DyDOC) and quantities passed among these. DOC = Dissolved Organic Carbon.**

792 **Figure 2. Trajectories of deposition rates of: a) total reactive nitrogen, $\text{g N m}^{-2} \text{yr}^{-1}$; b) total sulphate, meq(-)**
793 **$\text{m}^{-2} \text{yr}^{-1}$; c) total chloride, $\text{meq(-)} \text{m}^{-2} \text{yr}^{-1}$; and d) total base cations (Ca, Mg, K and Na), $\text{meq(+)} \text{m}^{-2} \text{yr}^{-1}$, on**
794 **control (Con), acidified (Acid) and alkalisied (Alk) treatments, on peat and podzol (Pod) on the Migneint (Mig)**
795 **and Peak District (Peak) experimental sites.**

796 **Figure 3. Observations (symbols) and predicted trajectories of change (lines) in pH and dissolved organic carbon**
797 **(g C leached $\text{m}^{-2} \text{yr}^{-1}$) following additions from 2008 of rainwater ("Control"; ANC $-188 \text{ meq m}^{-2} \text{yr}^{-1}$ in**
798 **2010), alkalisng solution (ANC $+258 \text{ meq m}^{-2} \text{yr}^{-1}$ in 2010), and acidifying solution (ANC $-396 \text{ meq m}^{-2} \text{yr}^{-1}$ in**
799 **2010) to two soil types on each of two sites: a) Migneint peat; b) Migneint podzol; c) Peak District peat; d)**
800 **District podzol. Details of the experiment are given in Evans et al. (2012b).**

801 **Figure 4. Comparison of annual measurements 2008-2011 on two experimental sites with values predicted**
802 **by MADOC for: a) pH; and b) dissolved organic carbon (g C leached $\text{m}^{-2} \text{yr}^{-1}$), in control (triangles; "Con"),**
803 **acidified (squares; "Acid") and alkalisied (circles; "Alk") treatments, on each of two soil types: peat (filled**
804 **shapes) and podzol (outline shapes; "Pod"). The model was fitted to data from the control treatments.**
805 **Equivalence (1:1) plots are shown as dotted lines.**

806 **Figure 5. Observed (dots) and predicted (lines) values for: a) pH and b) DOC at an example Acid Waters**
807 **Monitoring Network site (Dargall Lane).**

808 **Figure 6. Comparisons of mean measured values with mean MADOC predictions for the period 1988-2010,**
809 **across all Acid Waters Monitoring Network sites: a) pH; b) dissolved organic carbon (DOC) flux, $\text{g C m}^{-2} \text{yr}^{-1}$;**
810 **and comparisons of observed with predicted rate of change for the period 1988-2010: c) pH, pH units yr^{-1} ; d)**
811 **DOC flux, $\text{g C m}^{-2} \text{yr}^{-1}$. Equivalence (1:1) lines are also shown.**

812 **Figure 7. Sensitivity to different combinations of N and S deposition (during the period 2020-2100), of a**
813 **range of modelled chemical variables: a) pH; b) dissolved organic carbon, $\text{g C m}^{-2} \text{yr}^{-1}$; and c) net primary**
814 **productivity, $\text{g C m}^{-2} \text{yr}^{-1}$. Outputs shown here were simulated by the MADOC model for the Migneint Podzol**
815 **site (control treatment), in 2021 (top row) and in 2100 (bottom row).**

816 **Figure 8. Sensitivity to different combinations (during the period 2020-2100) of mean annual temperature**
817 **and precipitation surplus, of a range of modelled chemical variables: a) pH; b) dissolved organic carbon**
818 **(DOC); c) dissolved organic nitrogen; and d) net primary production. Outputs shown here were simulated by**
819 **the MADOC model for the Migneint Podzol site (control treatment), in 2021 (top row) and in 2100 (bottom**
820 **row).**

821 **Figure 9. UK peat bogs: spatial distributions in 2007 of: a) S deposition; b) N deposition, and of predictions**
822 **by the MADOC model of: c) pH; and d) dissolved organic carbon flux, $\text{g C m}^{-2} \text{yr}^{-1}$.**

823 **Figure 10. Alternative future trajectories of DOC flux following an increase in response to a rise in pH,**
824 **assuming that turnover of the PDOC pool is rapid (solid line) medium (dashed line) or slow (dotted line), as a**
825 **result of differences in the proportion of decomposition that becomes PDOC (k_{inpdC}) and in the proportion of**
826 **PDOC mineralised per year (k_{minpd}).**

827

828

829 Figures

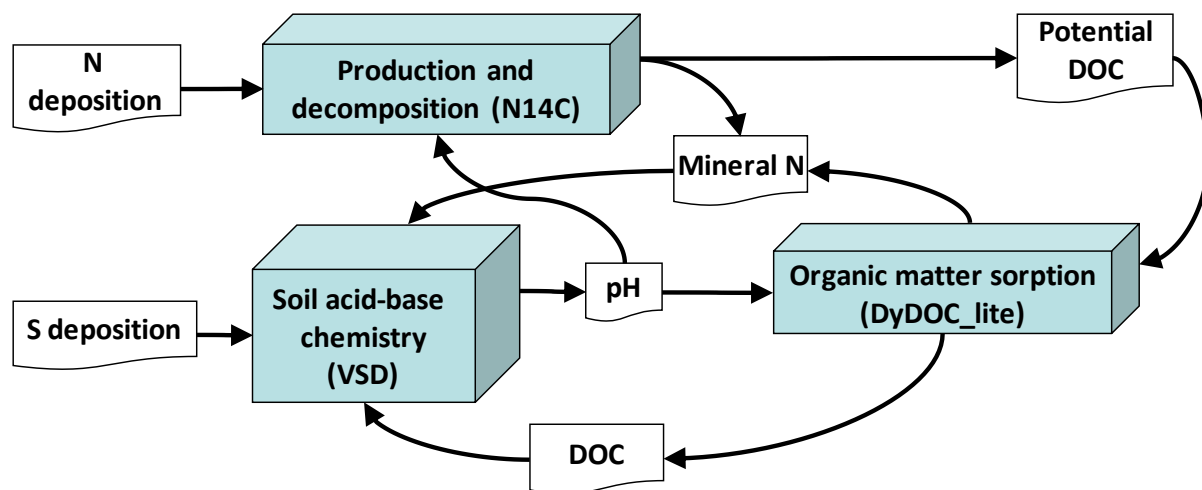
830

831 Figure 1.

832

833

834



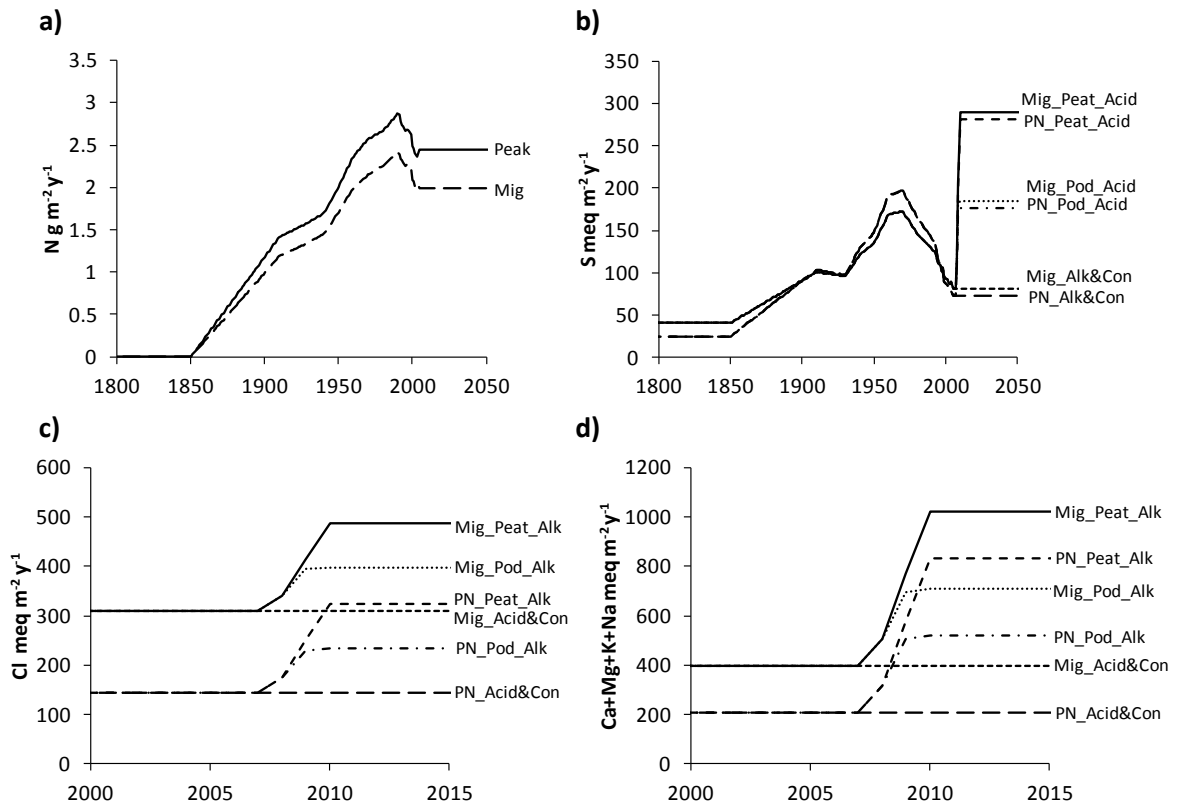
835

836

837

838
839 **Figure 2.**

840
841
842



843
844

845
846
847

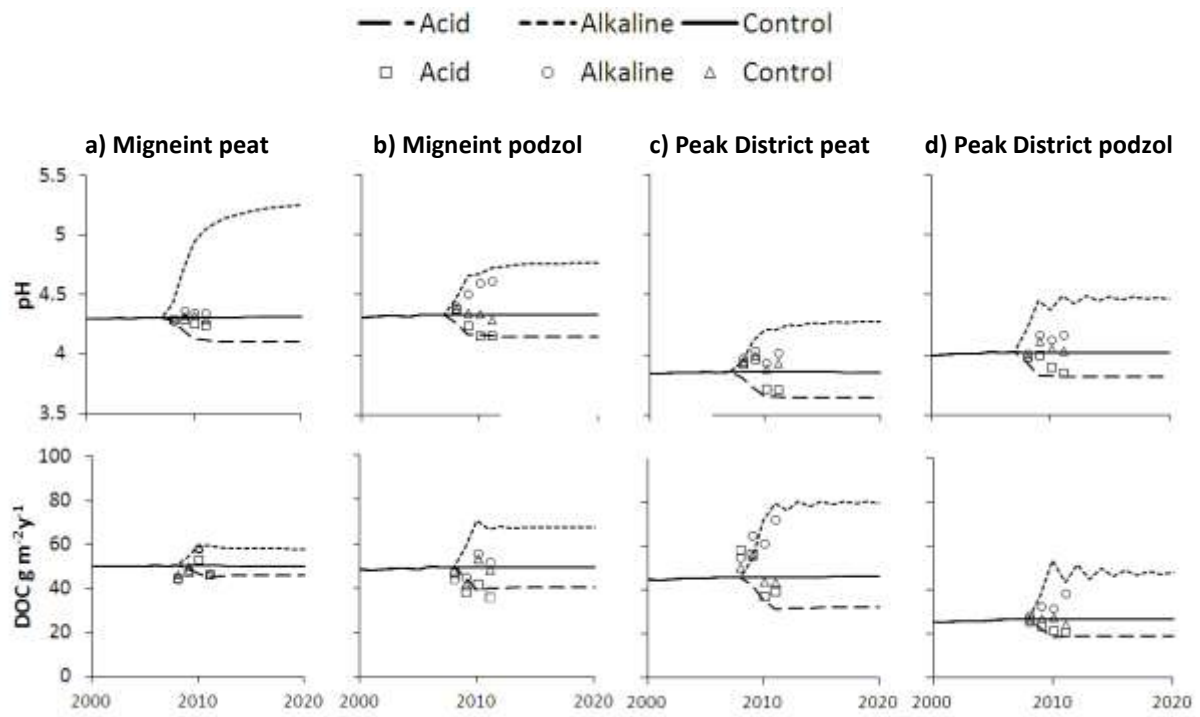
848

849 **Figure 3.**

850

851

852



853

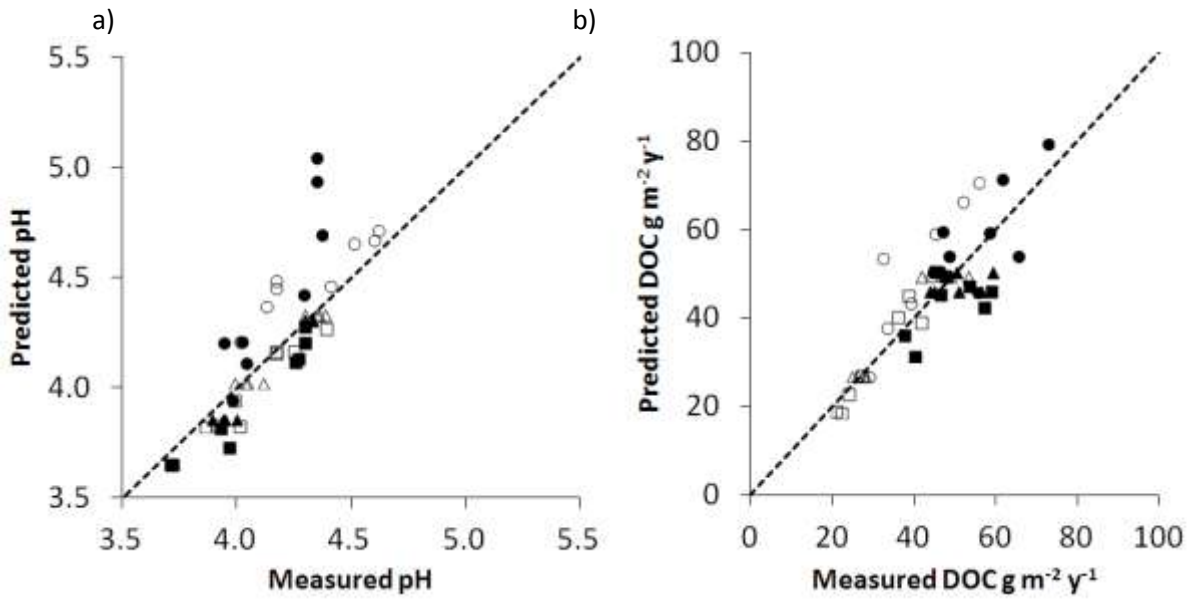
854

855

856

857
858
859
860

Figure 4.



861
862

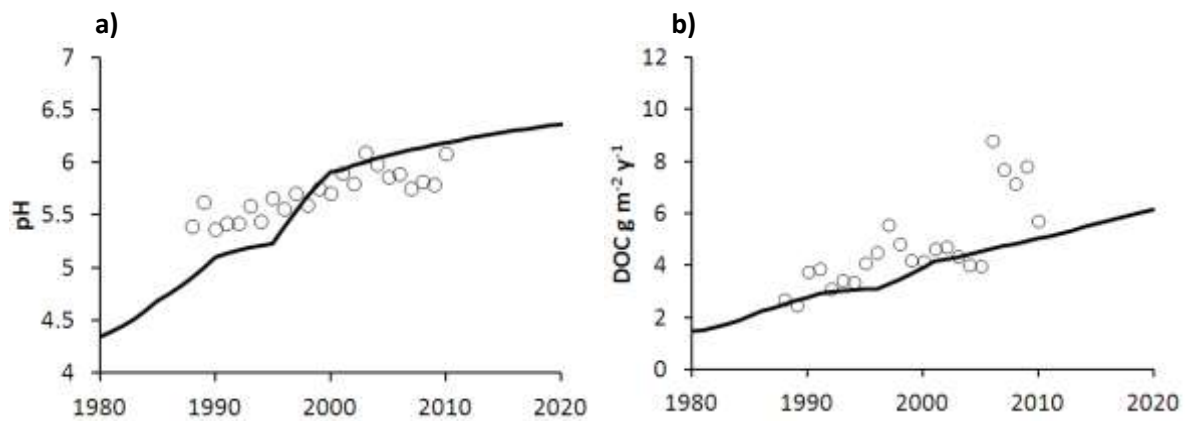
863
864
865

▲ Peat_Con ■ Peat_Acid ● Peat_Alk
△ Pod_Con □ Pod_Acid ○ Pod_Alk

866

867 **Figure 5.**

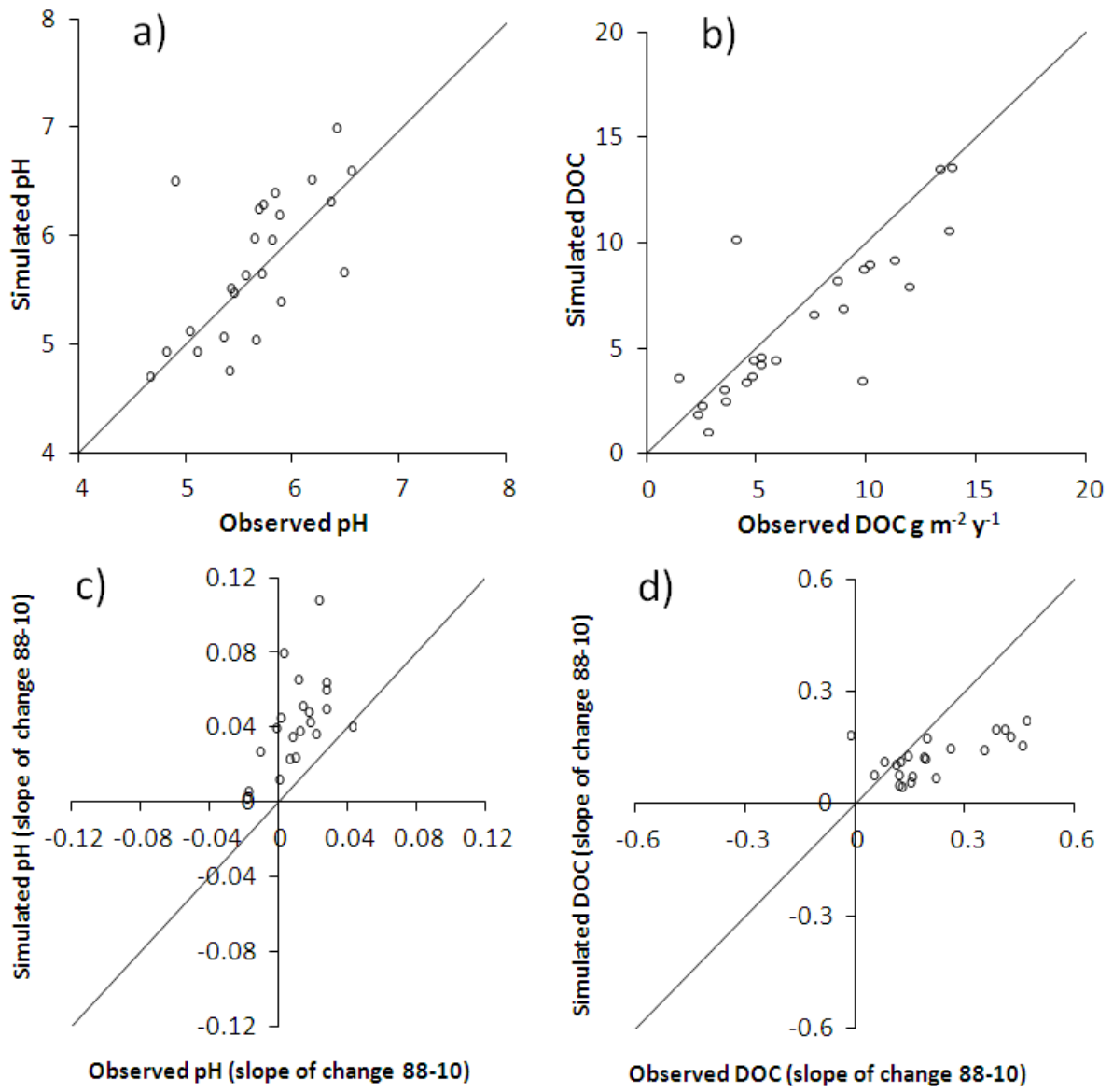
868



869

870

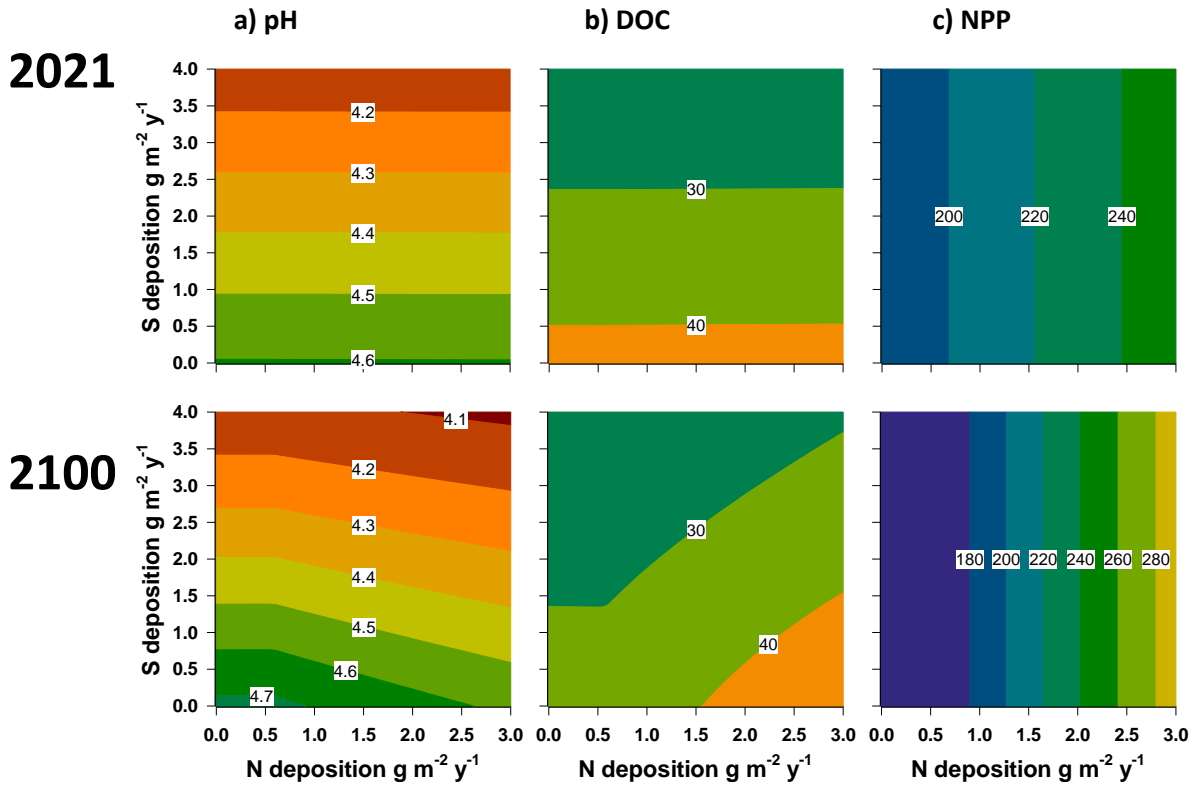
871
872 **Figure 6.**
873



874
875

876
877 **Figure 7.**

878
879



880

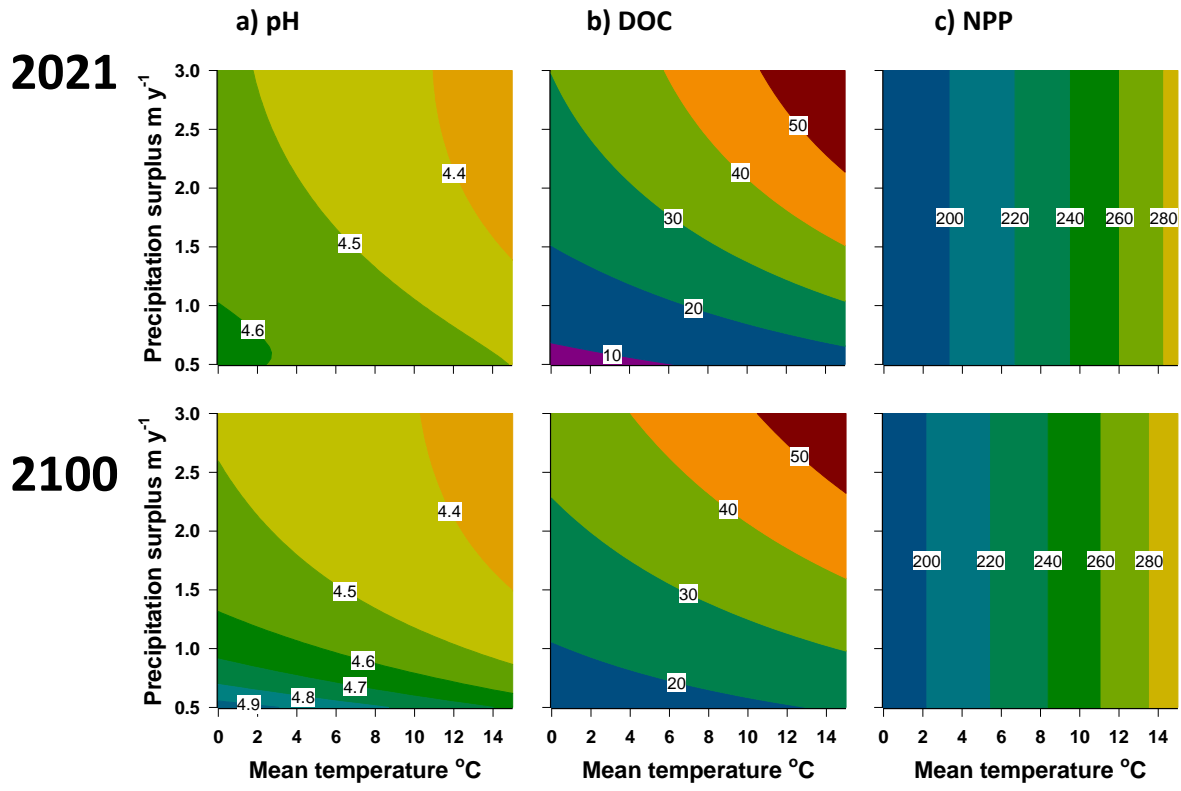
881
882
883

884

885 **Figure 8.**

886

887

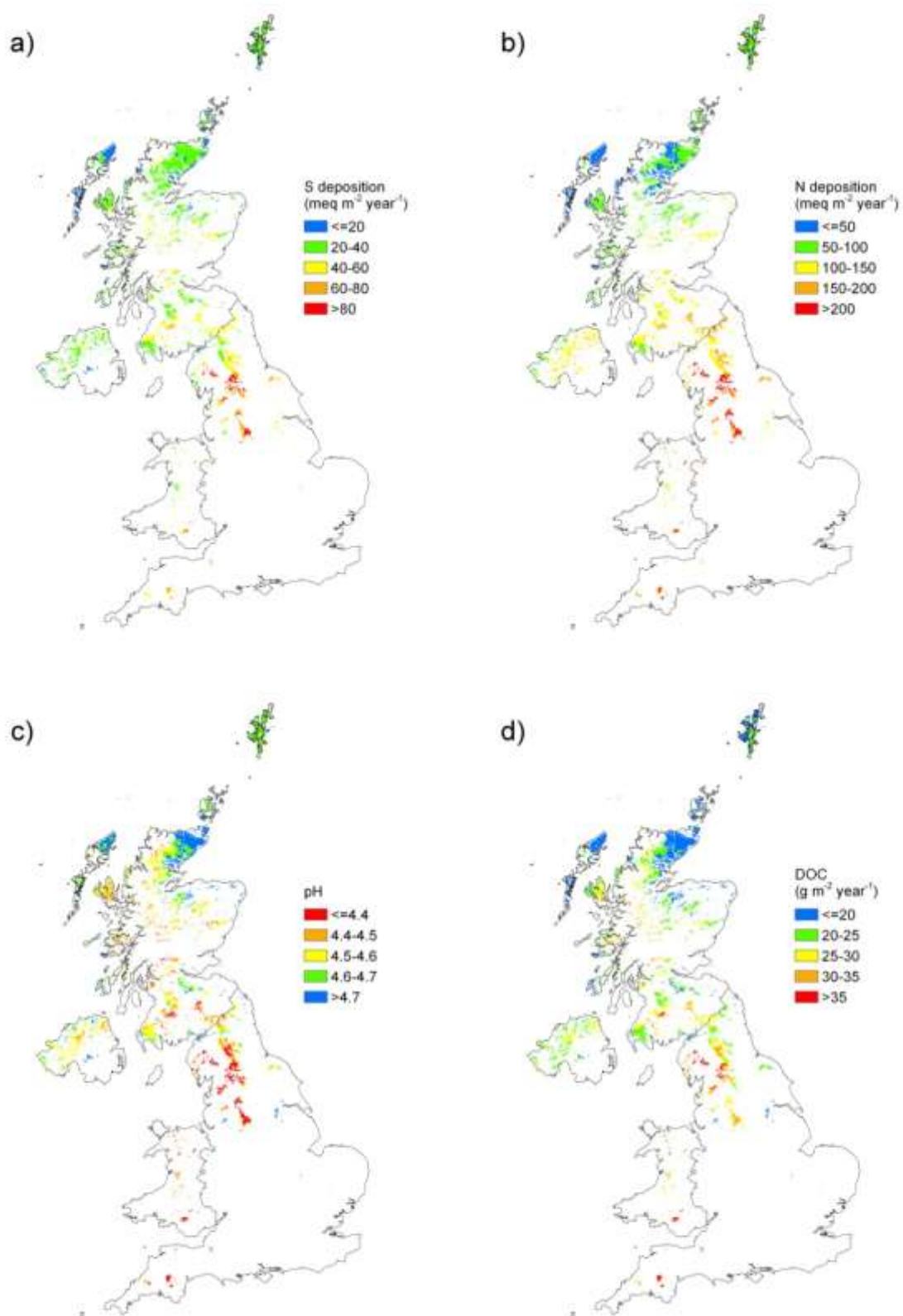


888

889

890

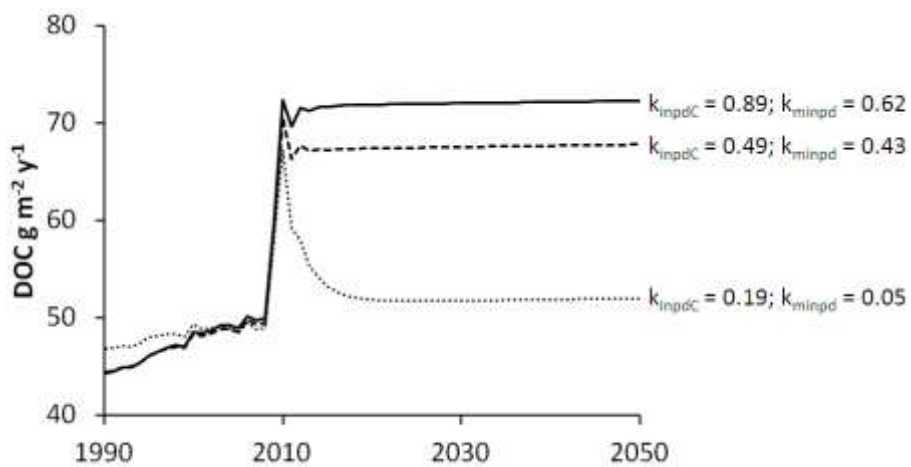
891 Figure 9.



892

893
894

895
896 **Figure 10.**
897



898
899
900
901
902
903
904